NXT-CAL-107

Rev. (-)

Report on the Proton Calibration of HEPAD SN 002 Consisting of HEPAD: FAC PN 571774-01, Serial No. 002 at the Alternating Gradient Synchrotron of Brookhaven National Laboratory

June 6, 1990

Prepared for

Ford Aerospace Corporation
Space Systems Division
Bldg. 3, 3825 Fabian Way
Palo Alto, California 94303

by

PANAMETRICS, INC.
221 Crescent Street
Waltham, Massachsetts 02254

HEPAD Project Engineer	Paul R. Morel	Date	6/6/90
Product Assurance	[signature]	Date	6/6/90
Configuration Management	Norm Arsenault	Date	6/6/90
Program Physicist	Frederick A. Hanser	Date	6/6/90
Program Manager	B. Sellers	Date	6/6/90

TABLE OF CONTENTS

LIST OF FIGURES

LIST OF TABLES

1. INTRODUCTION

The HEPAD SN 002 unit was calibrated in detail at the Brookhaven National Laboratory Alternating Gradient Synchrotron. A time-of-flight (TOF) system supplied by the Aerospace Corporation was used to select narrow energy width proton beams from a broader magnet-selected proton beam. The TOF system was implemented to eliminate spurious secondary proton energy responses and provided good proton energy selection for the HEPAD calibration.

The HEPAD responses were measured as outlined in the Calibration Plan of Ref. 1. The angular response measurements at high energy show that the 12° HEPAD response is, to within 5-10%, an approximation of the omnidirectional response. A detailed calibration of the HEPAD SN 002 was made with the instrument at 12° with respect to the beam, using both the proton channels (P8 to P11) and the photomultiplier tube analog output pulse height spectra. The 12° HEPAD response to the accelerator relativistic beam is equal to the instrument's response to the zenith view atmospheric muons to within 5-10%. The lower energy proton channels, P8 and P9, have a response to rear entry high energy protons. The rear entry response to the relativistic beam is in good agreement with the nadir view atmospheric muon response.

The details of the experimental configuration at the Brookhaven accelerator, and a list of energies and angles where data were taken, are presented in Section 2. Analysis of the accelerator data and test results are in Section 3. Section 4 contains the summary of the HEPAD SN 002 atmospheric muon tests.

2. EXPERIMENTAL CONFIGURATION AT BNL AND LIST OF DATA OBTAINED

In February, 1990, the HEPAD SN 002 unit was calibrated at the A2 Test Beam of the Brookhaven National Laboratory (BNL) Alternating Gradient Synchrotron (AGS) accelerator. The response of the HEPAD,under bombardment by protons, with energies from 300 to 1,365 MeV, and highly relativistic pions and muons, was studied as a function of particle velocity and HEPAD orientation with respect to the beam axis. The experimental configuration is essentially as described in Ref. 1, with the basic setup identical to the one shown in Figure 2.1, except that three scintillator detectors were used instead of two shown in the figure.

A time-of-flight (TOF) system, using three thin plastic scintillator detectors, was used to select protons in an energy range much narrower than that provided by the beam line magnet system. The TOF scintillators were approximately 4"x4" (103.2 cm^2 area) and were centered on the beam line using reference marks on the A2 beam area floor. One scintillator was at the upstream end of the beam line, and two others were located approximately 40 ft downstream. The HEPAD was centered on the TOF scintillator area, using a laser to aid alignment, with the instrument's rotation pivot point approximately centered between the two solid state detectors (see HEPAD detector configuration, Figure 2.2).

The monitor detectors consisted of a 750 μm thick 2 cm^2 fixed position detector and a 1500 μm thick 0.25 cm^2 detector mounted on a linear scan device. During normal operation, both detectors were illuminated by the beam and the number of particles striking each detector during a data taking run was recorded for later use. At the beginning of the BNL testing, the monitor detectors were used to horizontally scan a 1,290 MeV proton beam to verify that the HEPAD was placed in a relatively uniform portion of the beam area. The results of the scan are plotted in Figure 2.3. Center of the HEPAD solid state detectors was located at the 0 cm location in the figure.

Particle counting was gated by a timer, usually set to 100 seconds. The S1, S2, S3, S4, S5, P8, P9, P10 and P11 HEPAD counts were recorded both with and without the requirement of a "good proton" TOF coincidence signal. "Good proton" signal required that all three TOF telescope scintillators were hit by a particle, and that the timing pattern of the hits showed that the proton had a certain well defined energy. The A7 and A8 counts were also

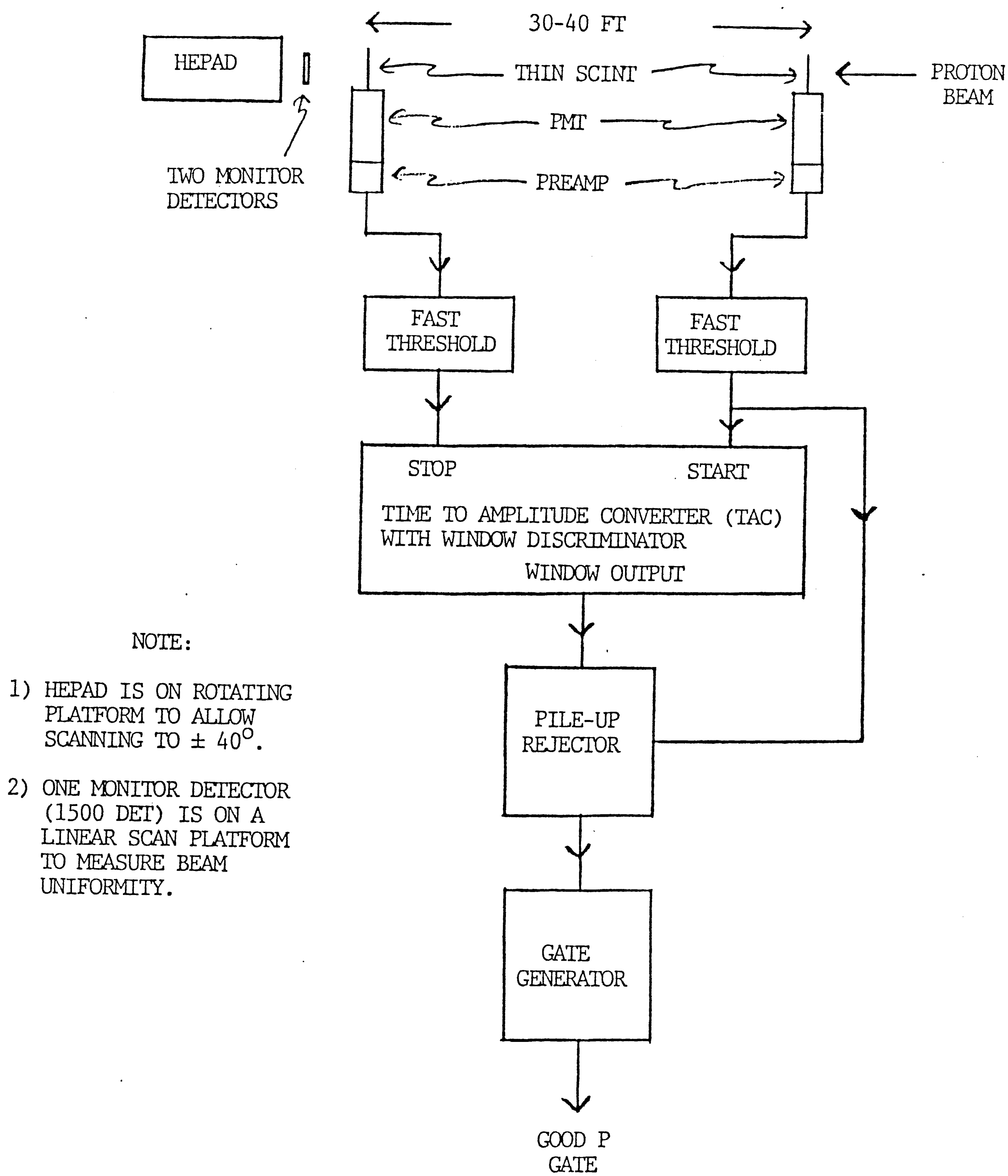

Figure 2.1 Basic Set-Up for the BNL AGS HEPAD Calibration.

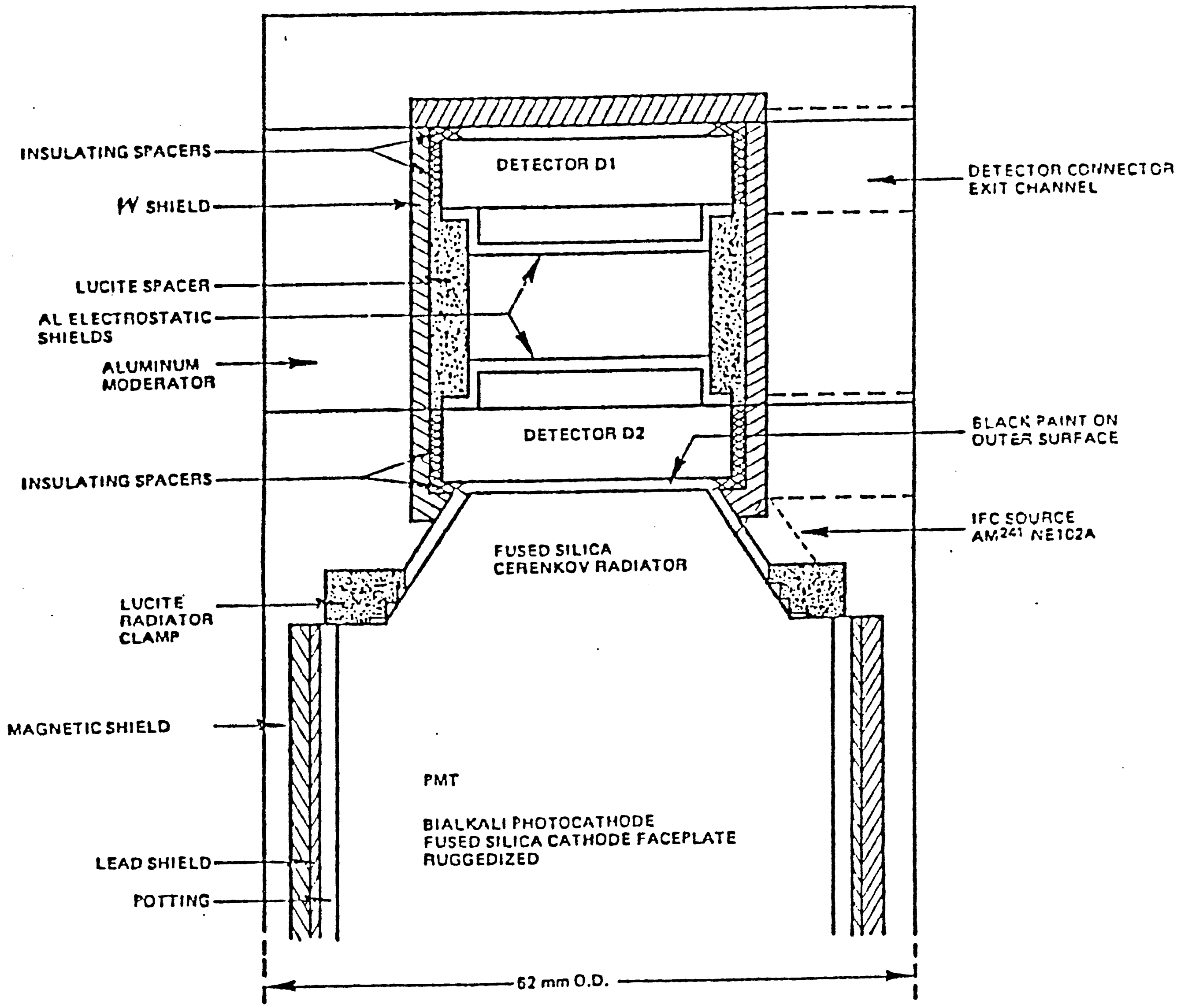

DETECTOR AREA: 3 cm^2
DETECTOR SEPARATION: 2.92 cm
GEOMETRIC FACTOR: G ≈ 0.9 cm^2-STER
ACCEPTANCE APERTURE: 68% OF G WITHIN < 24° HALF-ANGLE
100% OF G WITHIN < 34° HALF-ANGLE

Figure 2.2 HEPAD Telescope Subassembly - Detector End.

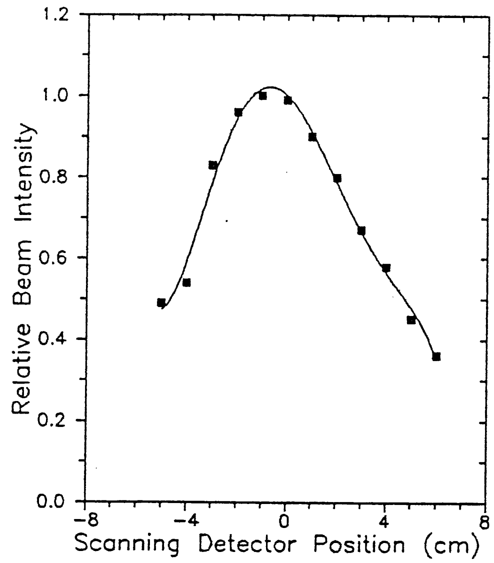

Figure 2.3 Beam intensity profile as measured by monitor detectors. Center of HEPAD was positioned in location corresponding to 0 cm. Line between the data points drawn to guide the eye.

recorded, but only without the TOF coincidence requirement. For each data run, the monitor detector counts, "good proton" TOF signals and the total number of TOF telescope events were recorded. In addition, the photomultiplier (PMT) pulse height spectrum was measured and recorded at each beam energy and angle using a computer based multi channel analyzer.

Most of the data were taken with the HEPAD at 12° with respect to the proton beam. The response at this angle has been found to be a good approximation to the omnidirectional response (Refs. 2 and 3). A list of the energies at which the 12° responses were measured is in Table 2.1. The data were taken with the HEPAD PMT at two different high voltage steps HV=37 and HV=35. The HEPAD angular response was measured at a number of energies. Table 2.2 contains the list of the energies and angles for both front and rear beam incidence runs.

Table 2.1 List of Energies of Measured 12° Responses		
Beam Energy (MeV)	Beam Energy Spread* (MeV)	HV step
323	11	37
335	7	35
352	9	37
361	4	35
375	15	37
404	19	37
422	12	35
436	10	35
450	18	37
500	8	35
506	26	37
519	7	35
548	28	37
606	52	37
659	40	37
680	8	35
724	7	35
770	15	37
932	79	37
935	64	37
997	83	37
1,020	64	37
1,290	117	37
1,365	107	37
Relativistic	-----	37

* Beam intensity was nearly uniform across the entire spread.

Table 2.2

Listing of Proton Angular Response Data Obtained

Beam Energy (MeV)	Front or Rear Incidence	Angles Measured
404	Front	0°,±12°,±24°,±36°
606	Front	0°, 12°, 24°, 36°
935	Front	0°, 12°, 24°, 36°
1,290	Front	0°, 12°, 24°, 36°
404	Rear	0°, 12°, 24°, 36°
590	Rear	0°, 12°, 24°, 36°
944	Rear	0°, 12°, 24°, 36°
1,341	Rear	0°, 12°, 24°, 36°
Rel.	Rear	0°, 12°, 24°, 36°

3. ANALYSIS OF DATA AND PRESENTATION OF RESULTS

This section contains the summary of the HEPAD calibration work done with the high energy protons at the Brookhaven National Laboratory (BNL) Alternating Gradient Synchrotron accelerator and with atmospheric muons at Panametrics' Waltham facility. The HEPAD angular resonse data are discussed in Section 3.1 and the 12° response in Section 3.2. Section 3.3 contains the rear entry data.

3.1 HEPAD Angular Response for Protons

The HEPAD S1 and S2 counts are the singles counts from the front and rear solid state detectors, respectively. As the HEPAD is rotated with respect to the beam by an angle θ, the effective detector area scales as cos(θ). The solid state detector responses can be normalized using the "good proton", GP, counts from the TOF telescope. The theoretical expression for the ratio of S1 or S2 counts to the GP counts, $Y_i(\theta)$, is given by

$$Y_i(\theta) = \frac{S1\ Counts}{GP\ Counts} = \frac{A_i}{A_{TOF}} \cdot \frac{\epsilon_i}{\epsilon_{TOF}} \cdot \cos(\theta)\,, \tag{3.1}$$

where, i = 1 or 2 denotes front or back detector values, respectively, A_i and A_{TOF} are the solid state detector and TOF telescope areas, ϵ_i is the detector-TOF telescope coincidence efficiency and ϵ_{TOF} is the correction for the non-uniform beam profile across the TOF telescope area (see Figure 2.3) and imperfect alignment of the three TOF telescope scintillator detectors. The TOF scintillators are 4" squares, which gives A_{TOF} = 103.2 cm^2, and $A_1 = A_2$ are 3.0 cm^2.

The measured and calculated values of Y_i are shown in Figure 3.1. Data points are taken from a set of runs, at a beam energy of 1,290 MeV, for angles between -36° and +36° with respect to the beam. The value of $\epsilon_i/\epsilon_{TOF}$ = 0.70, used in the calculation to obtain the best fit to the measured Y_i values, is in good agreement with the value of 0.77 calculated assuming a perfect coincidence efficiency, ϵ_i = 1.00, and the beam profile shown in Figure 2.3. The S1 and S2 measured responses are in good agreement with the expected responses.

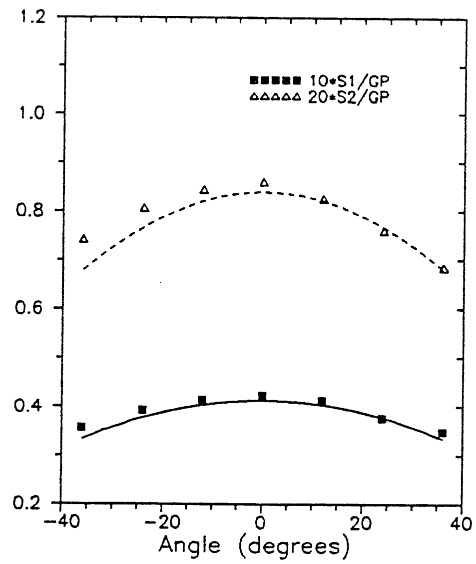

Figure 3.1 Measured and calculated values of Y_i. Lines show results of calculations using eq. (3.1).

Two other count rates of interest are the S5 rate, front-back solid state detector coincidence, and the total proton rate, P_{tot}, triple coincidence of the solid state detectors and the Cerenkov radiator. In terms of measured quantities, P_{tot} is the sum of the P8, P9, P10 and P11 count rates. The S5 and P_{tot} count rates can be normalized to the singles count rate of either one of the two solid state detectors.

The ratio of S5 or P_{tot} counts to S2 counts is given by

$$Y_{(5,P)}(\theta) = \frac{(S5,\ P_{tot})\ Counts}{S2\ Counts} = \frac{\epsilon_{(5,P)}A(\theta)}{A_2(\theta)} \qquad (3.2)$$

where subscripts 5 and P denote S5 and P_{tot} quantities, respectively, $A_2(\theta) = 3.00 \cdot \cos(\theta)\ cm^2$, ϵ is the coincidence circuit efficiency and $A(\theta)$ is the effective area subtended by the solid state telescope. For a coaxial set of two detectors of radius r and separated by a distance D, $A(\theta)$ can be written as

$$A(\theta) = 2r^2\cos(\theta)\,[\arccos(x) - x(1-x^2)^{1/2}], \qquad (3.3)$$

where

$$x = \frac{D}{2r} \cdot \tan(\theta) . \qquad (3.4)$$

For the HEPAD detectors r = 0.977 cm and D = 2.92 cm. The measured count ratios, as a function of angle, are plotted in Figure 3.2. The solid and dashed curves in Figure 3.2 are the S5 and P_{tot} ratios calculated using eq. (3.2) with $\epsilon_5 = 0.85$ and $\epsilon_p = 0.82$.

The HEPAD total effective geometric factor, G_{eff}, is given by

$$G_{eff} = \epsilon_P \int_0^{\theta_{max}} A(\theta) \sin(\theta)\, d\theta \quad , \qquad (3.5)$$

where ϵ_p is the triple coincidence efficiency, θ_{max} is the solid state detector telescope opening angle, and $A(\theta)$ is given by eq. (3.3). Evaluating the integral in eq. (3.5) yields

$$G_{eff} = \epsilon_P \frac{\pi^2}{2} \cdot [2r^2 + D^2 - D(4r^2 + D^2)^{1/2}] = 0.869\, \epsilon_P\, cm^2\text{-}sr \quad . \qquad (3.6)$$

The coincidence efficiency can be calculated most reliably using the 0° data. According to eq. (3.2), $\epsilon_p = Y_p(0°)$. Evaluating $Y_p(0°)$ at 404, 606, 935 and 1,290 MeV yields $\epsilon_p = 0.84 \pm 0.03$. The effective total HEPAD geometric factor is $G_{eff} = 0.73 \pm 0.03$ cm^2-sr.

At four energies, the HEPAD photomultiplier pulse height spectrum was measured as a function of angle. Three spectral quantities, peak channel, centroid channel and full-width-half-maximum (FWHM) for each energy and angle are listed in Table 3.1. In addition, the weighted average, over angle, of each quantity is also displayed in Table 3.1. The weights are 0.104, 0.518 and 0.359 for the 0°, 12° and 24° values, respectively. The weights are calculated using eq. (3.5) and assuming that the 0° spectrum represents data between 0° and 6°, the 12° spectrum represents the 6° to 18° data, and the 24° spectrum represents the data between 18° and 30°. It is evident that, for energies above 404 MeV, the 12° peak and centroid values are up to 9% larger then the weighted average values. Since the weighted average values are expected to closely approximate the true omnidirectional HEPAD response, a correction for this effect must be made when 12° data are used to construct the omnidirectional HEPAD response. A detailed discussion of this correction will be found in Section 3.2.

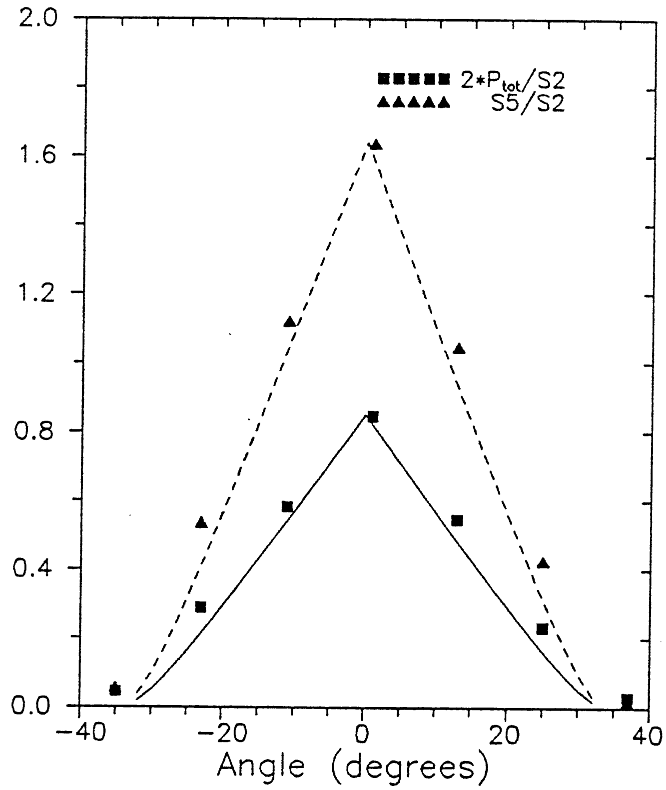

Figure 3.2 Measured and calculated S5 and P_{tot} to Good Proton ratios. Lines show results of calculation using eq. (3.2).

3.2 Calibration with Protons at 12° and Omnidirectional Response

The functional dependence of the PMT pulse height on the incident proton energy is shown in Figure 3.3. The beam energy is plotted against the ratio of the median pulse height to the relativistic beam pulse height. The solid curve is the taken from Ref. 3 and represents the calibration curve of previous HEPAD units. The dashed curves show $\pm 1\sigma$ spread of the PMT response. The old HEPAD calibration curve describes the current data very well, except in the region between 600 and 700 MeV. In this energy range, the slope of the previous calibration curve differs slightly from that of the new data, but is still within the $\pm 1\sigma$ limits.

The measured HEPAD area at 12° is listed in Table 3.2 and shown in Figure 3.4. The 12° HEPAD area, $A_{PMT}(12°)$, is calculated

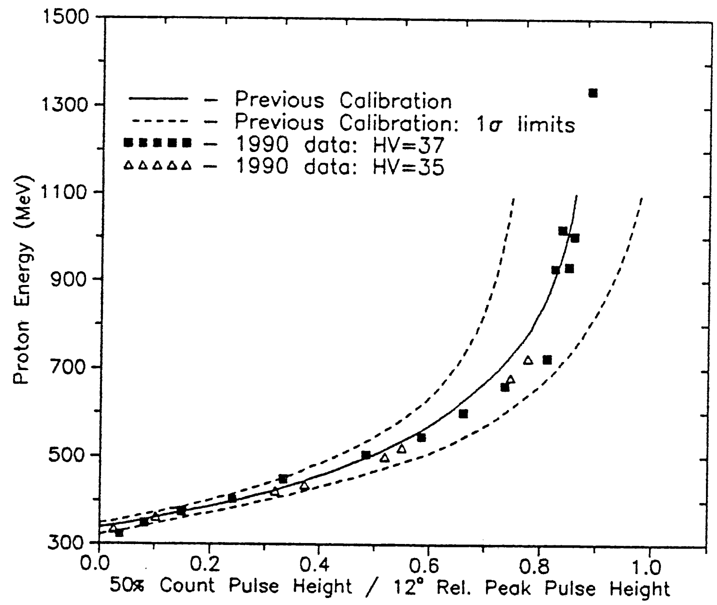

Figure 3.3 Proton beam energy plotted against the median pulse height from the phomultiplier analog output.

using

$$A_{PMT}(12°) = A_{S2} \cdot \cos(12°) \cdot \frac{P_{tot}\ Counts}{S2\ Counts} \tag{3.7}$$

where A_{S2} is 3.00 cm^2. The absolute magnitude of the PMT pulse heights, taken with the high voltage step 35, is smaller than those taken at the nominal operating high voltage step of 37. Therefore, the effective proton energy for an HV = 35 data point is lower than the beam energy. The correction term, needed to convert an HV = 35 beam energy to an equivalent beam energy for a HEPAD operating at HV = 37, is calculated in the following way. The HV = 35 pulse height to relativistic peak ratio is corrected for the lower gain by multiplying it by the ratio of the HV = 35 to HV = 37 relativistic peak ADC channels. The effective energy is then obtained from the curve shown in Figure 3.3; it is the energy that corresponds to the corrected pulse height ratio. The HV = 35 data points listed in Table 3.2 and plotted in Figure 3.4 include this energy correction. The 12° PMT area reaches its full value above for protons with energies above 400 MeV. The average value of the area above 400 MeV is 1.68 ± 0.16 cm^2.

Table 3.1

Summary of Data for HEPAD SN002 Angular Response for Protons

Angle (deg)	1290 MeV			939 MeV			606 MeV			404 MeV		
	Peak	Cent.	FWHM	Peak	Cent.	FWHM	Peak	Cent.	FWHM	Peak	Cent.	FWHM
0	1.23	1.20	0.19	1.05	1.05	0.15	1.03	1.02	0.24	0.90	0.93	0.32
12	1.00	1.04	0.24	1.00	1.01	0.19	1.00	1.01	0.22	1.00	1.04	0.40
24	0.89	0.90	0.14	0.82	0.82	0.15	0.80	0.84	0.24	1.10	1.04	0.47
Avg.	0.97	0.99	0.19	0.92	0.93	0.17	0.91	0.93	0.23	1.01	1.01	0.41

Notes:
1) Values normalized to the 12° peak at each energy.
2) Avg. is the weighted average of the 0°, 12° and 24° data.

Table 3.2

HEPAD PMT Area at 12° as Function of Proton Energy

Beam Energy (MeV)	HV step	Effective Energy (MeV)*	Area (cm^2)
323	37	323	0.31
335	35	330	0.76
352	37	352	1.51
361	35	355	1.55
375	37	375	1.38
404	37	404	1.56
422	35	415	1.78
436	35	430	1.71
450	37	450	1.57
500	35	490	1.82
519	35	504	1.87
506	37	506	1.84
548	37	548	1.78
606	37	606	1.84
680	35	631	2.05
659	37	659	1.70
659	37	659	1.80
724	35	665	1.87
770	37	770	1.81
932	37	932	1.73
935	37	935	1.74
997	37	997	1.67
1,020	37	1,020	1.66
1,290	37	1,290	1.62
1,365	37	1,365	1.63
Relativistic	37	Relativistic	1.47

* Effective energy includes the HV Step correction

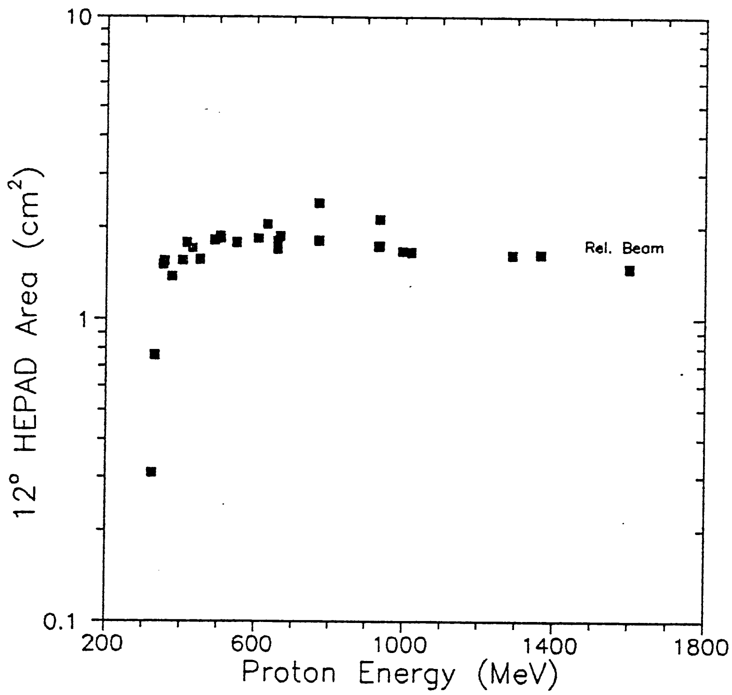

Firgure 3.4 Measured HEPAD area at 12° with respect to the beam.

The 12° response of the HEPAD to high energy protons has previously been used to represent the omnidirectional response (Ref. 3). As can be seen from the data in Table 3.1, the 12° PMT pulse height is approximately 9% larger than the corresponding average (omnidirectional) pulse height, for proton energies above 600 MeV. Consequently, an energy shift correction must be made in order to construct the omnidirectional response from the 12° data. The effective omnidirectional proton energy is obtained by multiplying the ratio of 12° PMT pulse height to the relativistic beam pulse height by 0.93 (for energies above 600 MeV), and finding the corresponding energy from the solid curve in Figure 3.1. The relative omnidirectional responses of the four proton channels (P8, P9, P10 and P11) are listed in Table 3.3 and are plotted in Figure 3.5. The nominal P8-P9, P9-P10 and P10-P11 breakpoint energies of 420, 510 and 700 MeV are also indicated in the Figure. It should be noted that the data in Table 3.3 and Figure 3.5 are valid only for an isotropic high energy proton flux. On orbit, the proton fluxes may not be isotropic but can be strongly directionally aligned by solar emission and the effects of the Earth's magnetic field lines. If the angle of incidence of the solar protons is known, then the HEPAD proton channel response can be calculated by interpolating the data in Table 3.1 for the angle required.

Table 3.3

Relative Omnidirectional Proton Channel Responses

Effective Energy (MeV)*	P8	P9	P10	P11
323	1.00	0.00	0.00	0.00
341	0.93	0.00	0.07	0.00
352	0.98	0.00	0.00	0.02
360	1.00	0.00	0.00	0.00
375	1.00	0.00	0.00	0.00
404	0.72	0.27	0.01	0.01
420	0.54	0.46	0.01	0.00
437	0.24	0.71	0.04	0.01
452	0.07	0.88	0.05	0.00
498	0.02	0.72	0.26	0.00
510	0.05	0.27	0.68	0.00
518	0.10	0.38	0.50	0.01
577	0.08	0.03	0.84	0.04
673	0.08	0.01	0.65	0.25
698	0.13	0.03	0.58	0.26
740	0.06	0.01	0.42	0.52
740	0.06	0.01	0.29	0.65
746	0.11	0.02	0.45	0.42
1205	0.05	0.01	0.10	0.85

* - Effective energy includes HV Step correction and correction for converting 12° response to omnidirectional response.

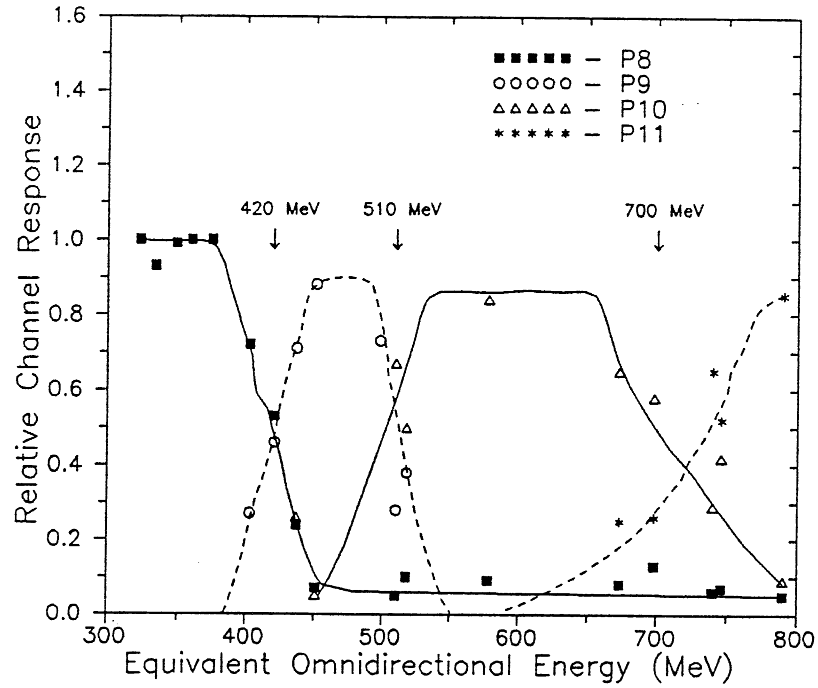

Figure 3.5 Relative responses of the P8, P9, P10 and P11 channels as a function of equivalent omnidirectional proton energy.

3.3 Rear Entry Proton Response

The HEPAD response to high energy rear entry protons was measured, as a function of angle at five beam energies. The angular responses of the solid state detectors (normalized to the "good proton" counts), including the S5 coincidence, are listed in Table 3.4. At all but the relativistic beam energy, the S1, S2 and S5 responses are slightly lower than the predicted values. This is primarily because of scattering and inelastic interactions in the shielding from the PMT, electronics and housing. The solid state detector responses are consistent with the front entry measurements, and are in rough agreement with the expected response when scattering and inelastic interactions are considered.

The only exception is the relativistic energy beam response which leads to S channel responses which are 40% too large. The probable reason for this discrepancy is that the geometric beam profile (see Figure 2.3) assumed for the relativistic beam is incorrect. If the relativistic beam has less angular dispersion than the measured 1,290 MeV beam then the relative efficiency

Table 3.4

Rear Entry Proton Data - S1, S2 and S5 Channels

Energy (MeV)	Angle (Deg)	Area (cm^2)				
		S1	S2	S1,S2 Theory	S5	S5 Theory
404	180	2.51	2.50	3.00	2.232	3.000
404	168	1.91	1.66	2.93	0.955	1.767
404	156	2.34	1.72	2.74	0.476	0.604
404	144	2.44	1.88	2.43	0.013	-----
590	180	2.51	2.42	3.00	2.202	3.000
590	168	2.33	1.99	2.93	1.258	1.767
590	156	2.45	2.08	2.74	0.599	0.604
590	144	2.54	1.93	2.43	0.028	-----
944	180	2.43	2.41	3.00	2.107	3.000
944	168	2.56	2.18	2.93	1.249	1.767
944	156	2.62	2.30	2.74	0.641	0.604
944	144	2.63	2.19	2.43	0.056	-----
1341	180	2.64	2.51	3.00	2.159	3.000
1341	168	2.41	2.26	2.93	1.248	1.767
1341	156	2.73	2.29	2.74	0.626	0.604
1341	144	2.64	2.14	2.43	0.076	-----
Rel	180	3.60	3.33	3.00	2.752	3.000
Rel	168	3.42	3.10	2.93	1.783	1.767
Rel	156	3.54	2.99	2.74	0.899	0.604
Rel	144	3.25	2.67	2.43	0.206	-----

Table 3.5

Rear Entry Proton Data - HEPAD Proton Channels

Energy (MeV)	Angle (Deg)	Area (cm^2)				
		P8	P9	P10	P11	P_{tot}
404	180	0.000	0.000	0.000	0.000	0.000
404	168	0.013	0.000	0.000	0.000	0.013
404	156	0.000	0.000	0.000	0.000	0.000
404	144	0.000	0.000	0.000	0.000	0.000
590	180	0.138	0.000	0.000	0.000	0.138
590	168	0.178	0.000	0.000	0.000	0.178
590	156	0.292	0.000	0.000	0.000	0.292
590	144	0.006	0.000	0.000	0.000	0.006
944	180	0.286	0.007	0.000	0.000	0.293
944	168	0.375	0.004	0.001	0.000	0.380
944	156	0.536	0.029	0.000	0.000	0.565
944	144	0.024	0.000	0.000	0.000	0.024
1341	180	0.521	0.007	0.003	0.000	0.531
1341	168	0.511	0.016	0.002	0.000	0.529
1341	156	0.431	0.120	0.001	0.000	0.552
1341	144	0.019	0.005	0.000	0.000	0.025
Rel	180	1.421	0.051	0.034	0.011	1.516
Rel	168	1.176	0.076	0.039	0.017	1.308
Rel	156	0.351	0.265	0.081	0.017	0.713
Rel	144	0.030	0.031	0.017	0.009	0.085

factor $\epsilon_i/\epsilon_{TOF}$, used in eq. (3.1) can be smaller than the value of 0.7 which is used to calculate the values in Table 3.4.

The HEPAD proton channel responses are listed in Table 3.5. The PMT pulse height response to the relativistic energy beam is too high for the proton channels just as it was for the solid state detector channels. At a proton energy of 1,341 MeV, the HEPAD response is nearly independent of angle, while below that energy, the response is peaked near 156°. The P8 channel response decreases rapidly at energies below 590 MeV. The P9 channel response is already very small at 944 MeV. The P10 and P11 channel responses can be neglected at all but highly relativistic energies. The measured rear entry properties of the HEPAD are in good agreement with those measured for previous HEPAD units (Ref. 3).

4. HEPAD RESPONSE TO ATMOSPHERIC MUONS

The response of the HEPAD SN 002 to atmospheric muons was measured five times between October, 1989 and March 1990. Both Zenith viewing (front entry) and Nadir viewing (rear entry) runs were made. Prior to and just following each atmospheric muon run, an α lamp spectrum was taken to verify proper operation of the HEPAD.

The data from Zenith view runs is summarized in Table 4.1, where the five runs are labelled by the date at the start of the test. The α lamp peak is approximately 0.34 of the atmospheric muon peak pulse height, with a full width at half maximum (FWHM) of about 50%. The average pulse height due to atmospheric muons ("μ avg., position" in Table 4.1) is 4-5% larger than the peak pulse height, indicating that the PMT pulse height spectrum is slightly asymmetric. The bulk of front entry atmospheric muon events are recorded in the P11 channel as is to be expeced for highly relativistic particles. The data in Table 4.1 show stable operation of the instrument between 10/89 and 3/90.

HEPAD data from the nadir view runs is summarized in Table 4.2. Comparison of the front and rear entry event rates shows that the effective HEPAD area for rear entry highly reltivistic particles is approximately 86% of that for front entry particles. The observed count rates show that the P8 and P9 channels are the ones most likely to be affected by rear entry particles.

Table 4.1

HEPAD SN 002 - Atmospheric Muon Runs - Zenith View

	Date of Atmospheric Muon Run					Average
	11/1/89	11/17/89	1/15/90	2/20/90	3/5/90	
α peak, position[1]	0.323	0.347	0.355	0.344	0.349	0.344
α peak, FWHM[1]	0.183	0.173	0.183	0.174	0.173	0.177
μ peak, FWHM[1]	0.300	0.373	0.266	0.251	0.283	0.295
μ avg., position[1]	1.032	1.057	1.055	1.033	1.035	1.043
μ peak, 2.36σ[1]	0.353	0.365	0.340	0.357	0.373	0.358
Total Count Rate[2]	0.549	0.581	0.534	0.521	0.581	0.553
P11 Rate/Total Rate	0.909	0.952	0.918	0.893	0.885	0.911

Notes: 1) Normalized to the atmospheric muon peak pulse height

2) Atmospheric muon counts/minute

Table 4.2

HEPAD SN 002 - Atmospheric Muon Runs - Nadir View

	Date of Atmospheric Muon Run					Average
	11/1/89	11/17/89	1/15/90	2/20/90	3/5/90	
P8 Rate/Total Rate	0.702	0.715	0.670	0.701	0.704	0.698
P9 Rate/Total Rate	0.177	0.178	0.205	0.209	0.193	0.192
P10 Rate/Total Rate	0.070	0.059	0.075	0.060	0.062	0.065
P11 Rate/Total Rate	0.051	0.047	0.051	0.030	0.042	0.044
Total Rate (cnts/min)	0.462	0.480	0.460	0.430	0.472	0.461

REFERENCES

1) Proton Calibration Plan for HEPAD at the Alternating Gradient Synchrotron of Brookhaven National Laboratory, Panametrics, Inc., PANA-NOAA-TP2 (March 25, 1986).

2) M. C. Rinehart, Cerenkov Counter for Spacecraft Application, NIM, **154**, 303 (1978).

3) Report on the Proton Calibration of HEPAD's SN6 and SN9 at the Alternating Gradient Synchrotron of Brookhaven National Laboratory, Panametrics, Inc., PANA-NOAA-CAL1 (August 5, 1986).